Experimental Determination of Changes in Conductivity with Electric Field, Using a Stationary High-Field Domain Analysis*

K. W. Böer, G. Döhler,† G. A. Dussell, and P. Voss
Physics Department, University of Delaware, Newark, Delaware 19711
(Received 4 December 1967)

A method is described to determine experimentally the conductivity as a function of the actual electric field at high fields in the range of negative differential conductivity. For CdS doped with Ag and Al, it is shown that the conductivity decreases from about 10^{-7} to below 10^{-10} Ω^{-1} cm^{-1} at fields from 20 to 200 kV/cm. The experimental method is discussed by analyzing solutions of the Poisson and transport equations in terms of their projections in the n-E plane, by following along the field of directions.

1. INTRODUCTION

HIGH-FIELD effects observed in solids, e.g., the Stark effect, the Franz-Keldysh effect, field excitation of trapped charges, prebreakdown excitation, and electroluminescence, are determined by the actual field distribution in a crystal. It is well known that the assumption of a homogeneous field usually leads to wrong values of the actual field. Doping inhomogeneities, space-charge regions close to the electrodes, and field instabilities are known causes for marked field inhomogeneities.

For quantitative analysis the knowledge of the field distribution, i.e., of the value of the field strength at any position in the crystal, is essential. However, such knowledge could not be obtained to satisfaction with any known method. Electrode probing reveals only the potential distribution along the surface of a crystal, and it is restricted to low- and medium-field strength ranges (because of discharge along the surface at higher applied voltages). Franz-Keldysh-effect[1,2] probing yields information about the field distribution in the bulk, but has not allowed a quantitative determination because of a lack in reliable calibration.

It is the purpose of this paper to show that, in crystals with stationary steplike field domains[3–11] occurring in a range of negative differential conductivity, the high- and low-field values can be quantitatively determined, and the conductivity can be obtained as a function of the actual field.

2. STATIONARY STEPLIKE FIELD DOMAINS

It has been shown that stationary solutions of the Poisson and transport equations[12]

$$\frac{dE}{dx}=\frac{e}{\epsilon\epsilon_0}\rho(n,E),$$
$$\frac{dn}{dx}=\frac{1}{\mu kT}(e\mu nE-j) \tag{1}$$

may have a steplike character, provided that there is a range of negative differential conductivity and that the applied voltage is high enough.[3,4,7] (n is the density of conduction electrons, μ the mobility, j the current, E the field strength, and ρ the space charge.)

The solutions of this system can be instructively discussed in terms of their projections into the n-E plane, following the field of directions, since Eq. (1) represents an autonomous system.[13] This field of directions, as given by dn/dE, changes sign at the zeros of Eq. (1). Therefore two auxiliary functions, $n_1(E)$ given by $\rho(n_1,E)=0$, and $n_2(E)$ given by $e\mu n_2E-j=0$, divide the n-E plane into regions of different quadrants of the directions, symbolized by arrows in Fig. 1. These arrows "point towards" increasing x. Figures 1(a)–1(c) are drawn for three increasing values of the current.

For simplicity, a field-independent mobility is assumed in Fig. 1 and the following discussion.

Steplike solutions can occur if $n_1(E)$ has a range in which it decreases stronger than linearly with increasing field. Such solutions start close[14] to the singular point

* Supported by a grant from the Office of Naval Research, Washington, D. C.

† On leave of absence from Institut für Theoretische Physik II, University of Marburg, Germany.

[1] W. Franz, Z. Naturforsch. **12a**, 484 (1958).

[2] I. V. Keldysh, Zh. Eksperim. i Teor. Fiz. **34**, 1138 (1958) [English transl.: Soviet Phys.—JETP **6**, 788 (1958)].

[3] K. W. Böer, Phys. Rev. **139**, A1949 (1965).

[4] K. W. Böer and P. L. Quinn, Phys. Status Solidi **17**, 307 (1966).

[5] H. Kiess, Phys. Status Solidi **4**, 107 (1964).

[6] H. Kiess and F. Stöckmann, Phys. Status Solidi **4**, 117 (1964).

[7] G. Döhler, dissertation, Marburg, 1966 (unpublished); Phys. Status Solidi **19**, 555 (1967).

[8] V. I. Stafeev, Fiz. Tverd. Tela **5**, 3095 (1963) [English transl.: Soviet Phys.—Solid State **5**, 2267 (1964)].

[9] M. S. Kagan, S. G. Kalashnikov, and N. G. Zhdanova, Phys. Status Solidi **11**, 415 (1965).

[10] V. L. Bonch-Bruevich and S. H. M. Kogan, Fiz. Tverd. Tela **7**, 23 (1965) [English transl.: Soviet Phys.—Solid State **7**, 15 (1965)].

[11] M. Polke, Phys. Status Solidi **5**, 279 (1964).

[12] For simplicity, a model with only one relevant spatial coordinate (x) is discussed here. The space charge $\rho(n,E)$ is given by reaction kinetics, including field-dependent transitions.

[13] K. W. Böer and W. E. Wilhelm, Phys. Status Solidi **3**, 1704 (1963).

[14] As soon as the solution curve leaves the vicinity of the singular point, the field changes very rapidly with x, i.e., the transition range between E_{II} and E_I or E_{III} has a width of the order of the Debye length. Solutions extending over distances long compared with the Debye length must reach the vicinity of at least one singular point. [The Debye length is taken for the lowest $\rho(n,E)$ along the solution, outside the "vicinity" of the singular points.]

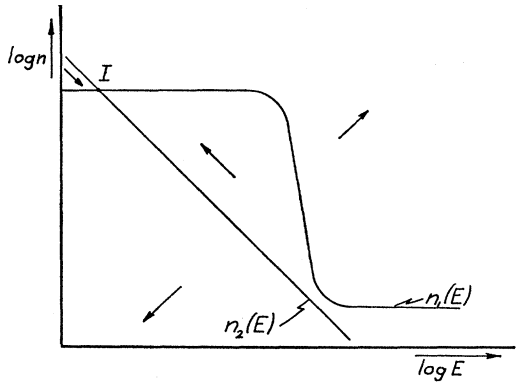

(a)

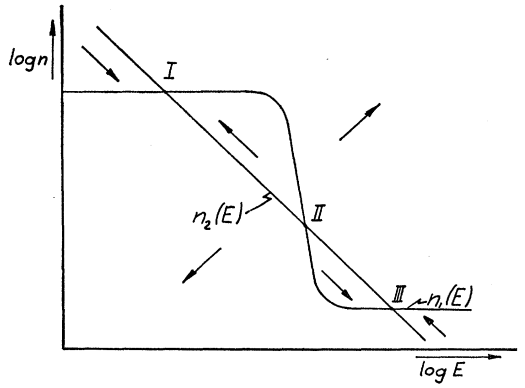

(b)

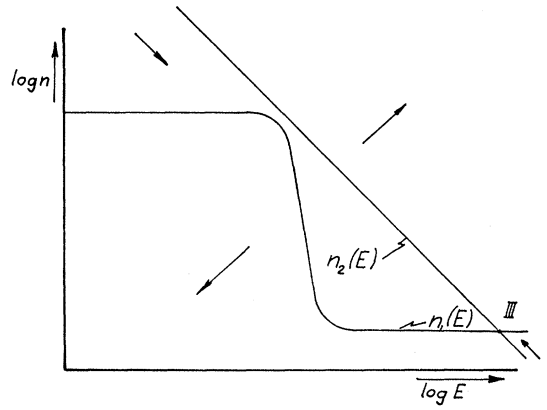

(c)

FIG. 1. Schematic field of directions with functions $n_1(E)$ and $n_2(E)$ for three values of the current [increasing j from (a) to (c)].

II and approach the singular points I or III, depending on the applied voltage,[5,15] and are indicated by heavy arrows in Fig. 2.

The electron concentration n_c at the cathode boundary[16] determines the starting point of the solution[7,15]

[15] K. W. Böer and P. Voss, Phys. Rev. (to be published).

[16] Cathode-adjacent steplike solutions cannot occur if $n_c > n_1(E \simeq 0)$, as can be seen from the field of directions (see, e.g., Fig. 2).

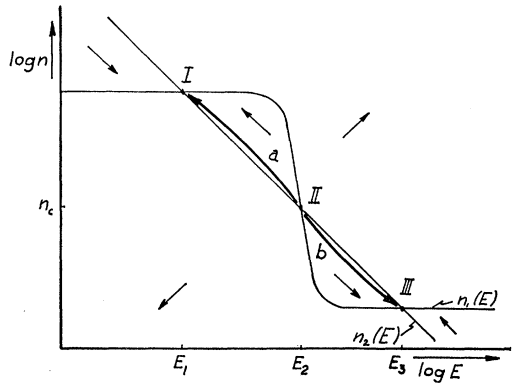

FIG. 2. Field of directions as given in Fig. 1(b) with steplike solutions, indicated by heavy arrows a and b.

and, for steplike solution, also approximately determines the current and the singular points ($n_c \simeq n_{II}$, the electron density at the second singular point).

Fields and electron densities at these singular points can be experimentally obtained by measuring the width d of the high-field domain as a function of the applied voltage V, using the approximations

$$E_{II}d + E_I(L-d) = V \tag{2a}$$

for cathode-adjacent high-field domains (a in Fig. 2) or

$$E_{III}d + E_{II}(L-d) = V \tag{2b}$$

for anode-adjacent high-field domains (b in Fig. 2); L is the length of the crystal between the electrodes, and

$$n_i = j/e\mu E_i, \tag{3}$$

with i=I, II, or III. The width of the domains can most easily be determined by using the Franz-Keldysh effect.

In actual practice, high-field domains adjacent to the anode are not easily obtainable, because of the tendency for very high fields to cause surface-glide discharges. Therefore usually only the values E_I, E_{II}, n_I, and n_{II} are available.

For determination of the $n_1(E)$ curve, one needs to vary the positions of the singular points, i.e., the current j. Since steplike domains require current saturation, the only way to change the current without changing $n_1(E)$ is to change the electron density at the cathode.[15]

This can be achieved by applying different metals as cathodes to the same homogeneously doped crystal.

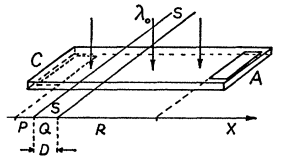

FIG. 3. Crystal platelet with electrodes (C and A) evaporated onto opposite surfaces, irradiated with band-edge light (λ_0), part of which is blocked off by a shadow S-S of a width D.

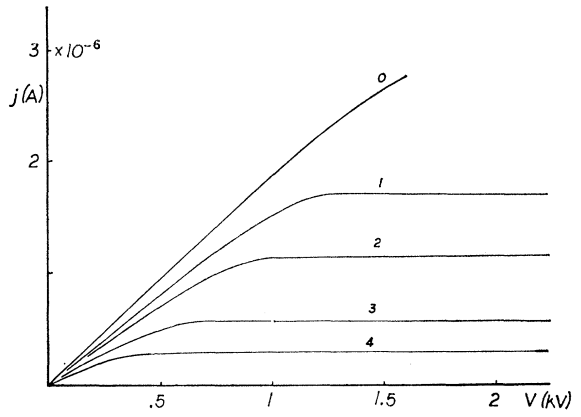

FIG. 4. Typical current-voltage characteristics of a CdS: Cu, Al platelet. (0) Homogeneously illuminated with 2×10^{12} photons/cm^2 sec at 507 nm, (1) with additional ir irradiation at 950 nm in region Q, (2) with additional stronger ir irradiation in Q, (3) with shadow in Q, (4) with shadow and ir irradiation in Q.

However, more conveniently, one can produce an artificially reduced electron concentration in a region of the bulk, which acts as a pseudocathode. This can be done in photoconductors with a shadow and/or a slit of infrared (ir) irradiation, the shadow or the ir-light slit being focused onto the crystal and shown by S-S in Fig. 3. Varying the light intensity in the shadow or ir-light slit region allows one to change n_s, the electron density in this region (Q in Fig. 3), and hence the boundary concentration in region R, the region in which steplike field domains will occur as long as n_s is smaller than n_c, the electron concentration at the actual cathode (boundary of region P).

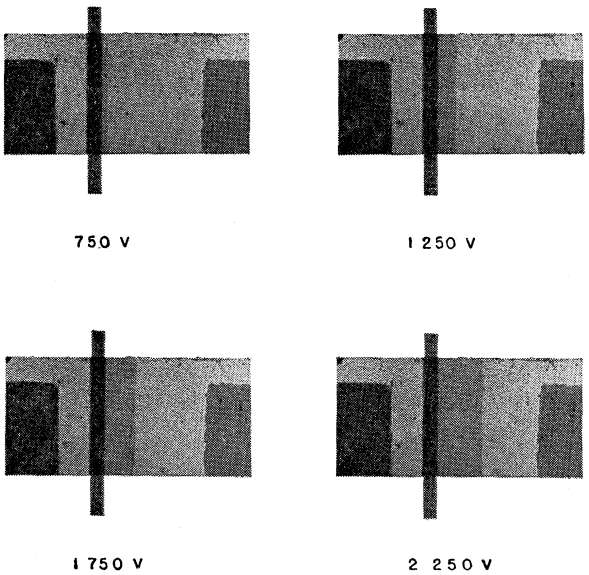

FIG. 5. Photographs in monochromatic light (507 nm) of CdS platelet with shadow, showing the high-field domain increasing in width in region R adjacent to the shadow, for increasing voltages applied to the crystal (cathode at the left side).

3. EXPERIMENTAL ARRANGEMENT

CdS single-crystal platelets grown by sublimation in an H_2S-N_2 atmosphere at about 1000°C and doped[17] with Ag and Al (about 50 parts per million) were used. "Ohmic" Ti/Al electrodes[18] were evaporated in a slit arrangement onto opposite surfaces (Fig. 3).

The crystal was mounted within a copper cavity for temperature variation and kept in a dry N_2 atmosphere. For the measurements reported, the crystal temperature was held constant at −65°C.

The crystal was illuminated with monochromatic light (2×10^{12} photons/cm^2 sec) at the band edge for Franz-Keldysh-effect observation and to produce photoconductivity. Photographs of the crystal were taken in band-edge light at 507 nm and used for further evaluations. The current-voltage characteristic was recorded, the voltage being measured at the crystal.

4. MEASUREMENTS

With the shadow in place, the applied voltage is increased. The current first increases linearly and then

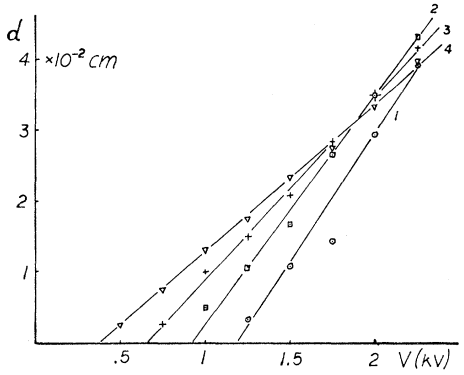

FIG. 6. Width d of the high-field domain as a function of the voltage applied to the crystal, for conditions corresponding to 1–4 in Fig. 4.

saturates (Fig. 4). The set of curves given in Fig. 4 is obtained by changing the added ir intensity in the shadow region Q from curve to curve. Curve O is the current-voltage characteristic without shadow or ir light.

As saturation occurs, a steplike high-field domain is observed in region R (Fig. 5). The width d of the domain increases linearly with applied voltage (see Fig. 6) and can be described by

$$V=ad+b, \tag{2c}$$

where a and b depend on the illumination in region Q, for constant illumination in P and R.

[17] The doping is done in order to obtain stationary high-field domains for applied voltages below the thermal breakdown.

[18] K. W. Böer and R. B. Hall, J. Appl. Phys. 37, 4739 (1966).

5. DISCUSSION

The experimental results indicate that high-field domains of a type described in Sec. 2 (type *a* of Fig. 2) occur in region *R*. Therefore one can obtain the values of E_{II} and E_I in the following way:

(1) The excess of the applied voltage over that at which saturation occurs, $V-V_S$, must[19] produce the excess field $E_{II}-E_I$ in the high-field domain:

$$V-V_S=(E_{II}-E_I)d, \qquad (2d)$$

where V_S is given by b and $E_{II}-E_I$ by a in Eq. 2(c).

(2) Using curve *O* (homogeneous case) in Fig. 4, the field E_I can be obtained from the voltage V_0 applied to the homogeneously illuminated crystal producing a current equal to the saturation current j_0, since this current lies in the ohmic range of curve *O*.

From Eq. (3) one can obtain n_I and n_{II} under the assumption of a field-independent mobility. For different illuminations in region *Q*, one can calculate a set of values for E_I, E_{II}, n_I, and n_{II}, and hence the $n_1(E)$ curve as given in Fig. 7. This figure includes three points obtained at high ir intensities for which saturation was not completely achieved at the highest applied voltage. The curve $n_1(E)$ in this region is dashed.

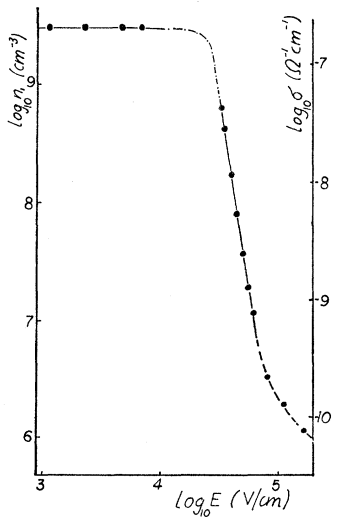

FIG. 7. Measured conductivity as a function of the actual electric field and neutrality density of conduction electrons $n_1(E)$, as calculated for a field-independent mobility of 500 cm²/V sec (at 208°K).

From the ohmicity of the current-voltage characteristic *O* in Fig. 4, one concludes that the mobility is field-independent in the entire measured range of n_I. However, for $E>17$ kV/cm (see Sec. 5 A), the mobility might change with the electric field, and therefore

[19] It will be shown in the following discussion (Sec. 5 A) that for current saturation, the voltage drop in region *P* and *Q* stays constant to a very good approximation with changing *V*.

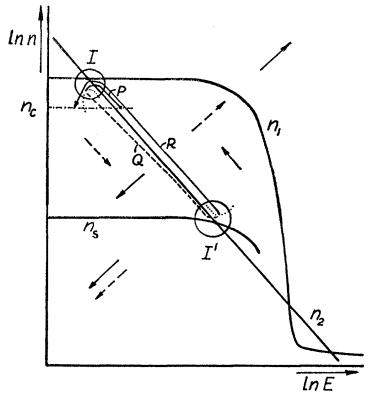

FIG. 8. Solution curve of the Poisson and current equation for an inhomogeneously illuminated crystal for "low" applied voltages (dashed part of the curve and dashed arrows in region *Q*). A discontinuity of slopes of the solution curve exists at the boundaries of region *Q* because of the assumed discontinuity of the optical excitation.

$n_1(E)$ may deviate somewhat from the given curve in the range of n_{II}. For correctness, the right-hand scale in Fig. 7 gives the measured values of the conductivity for the entire field-strength range ($\sigma_i E_i=j$, for $i=$I or II).

This curve gives the conductivity as a function of the actual field in the crystal, with only the assumption of a steplike domain. This assumption is sufficiently justified by the experimental observations given in Figs. 5 and 6.

A. Detailed Discussion of Continuous Solutions in an Inhomogeneously Illuminated Crystal

Earlier, it was assumed that the crystal can be represented by three regions, *P*, *Q*, and *R*, having approximately constant field distributions which do not change with applied voltage after a steplike domain occurs in region *R*; and that a value close to the singular

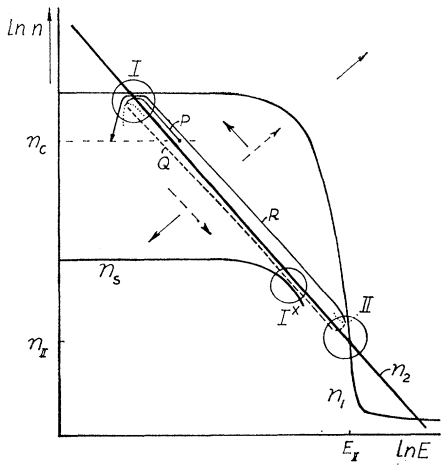

FIG. 9. Solution curve as in Fig. 8, however, for "high" applied voltages.

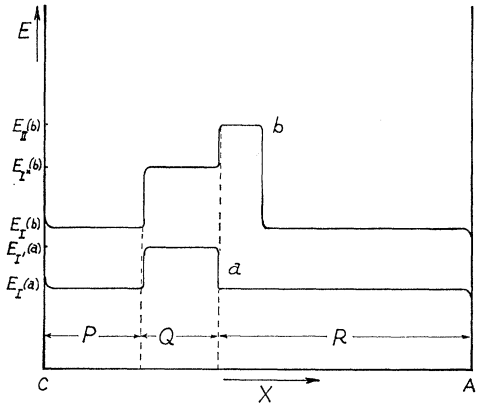

FIG. 10. Field distribution for an inhomogeneously illuminated crystal for low (*a*) and high (*b*) applied voltages. A high-field domain is formed in region R if the voltage is sufficiently high.

point (n_{II}, E_{II}) can be reached by the solution at the boundary between Q and R.

To justify this assumption, a detailed discussion of the continuous solution in the three regions P, Q, and R shall be conducted, following the outline of Sec. 2. A homogeneous optical excitation in each region shall be assumed for simplicity, the optical excitation in region P and R being the same, and the excitation in Q being reduced.

Figure 1 can also be read as the symbolized field of directions for different relative values of $n_1(E)$ and $n_2(E)$, $n_2(E)$ being constant (constant j) and the $n_1(E)$ values being decreased because of decreased optical excitation or increased quenching in Q.

For a crystal with regions of different optical excitations, the solution curve must satisfy Eq. (1) for every region separately, i.e., it must follow the corresponding field of directions. When going from one crystal region to the next, one proceeds from one field of directions to the field of directions appropriate for that region, however, conserving continuity of $n(x)$ and $E(x)$. Such a solution is pictured in Fig. 8 for low applied voltages in a crystal with a shadow region [$n_s(E)$ is $n_1(E)$ for the shadow region Q]. The solution starts in region P at n_c and a field value, selected by the applied voltage, moves close to the singular point I, crosses $n_2(E)$, and changes into region Q at the intersection with the dotted line.[20] Then the solution approaches the singular point I′, crosses $n_2(E)$ again, and enters region R at the second dotted line. Finally, the solution moves back close to the singular point I and then goes to n_a, the electron density at the anode (in Fig. 8, it is assumed $n_c=n_a$). The close proximity of the solution to the singular points is necessary to allow the solution to extend over dimensions long compared with the Debye length. Thus, practically homogeneous fields within the three regions are assured for regions long compared with the Debye length. This type of solution is the only one which can fulfill the given boundary condition, as can be seen from the fields of direction in Fig. 8.

It is evident from this discussion that the current and the solution curves are completely determined by n_c, n_a, and V for a crystal with a given illumination.[21]

Neglecting the voltage drop at the cathode and anode barrier and assuming steplike field distributions, justified above, and a field-independent mobility, n_s at I (Fig. 8) can be determined by

$$n_I/n_s=(L/D)(V/V_0-1)+1, \qquad (4)$$

where D is the width of the shadow (or slit), and V and V_0 are the applied voltages necessary to obtain the same current j with and without a shadow region, respectively [$j(V_0)$ being ohmic].

The current increases with increasing V until $n_2(E)$ no longer intersects with $n_s(E)$ for $E<E_{II}$ (Fig. 9), i.e., the singular point I′ in region Q disappears [see also Fig. 1(c)]. However, $n_2(E)$ and $n_s(E)$ must remain in close proximity (I* in Fig. 9) in order to allow a continuous set of stationary solutions with increasing V; therefore the current must saturate. The field in region Q can remain nearly constant, because $dn/dx \simeq dE/dx \simeq 0$ in the vicinity of I*. A further increase in V without an increase of j becomes possible, because the solution can now extend close to the singular point II (Fig. 9) and form a high-field domain in region R

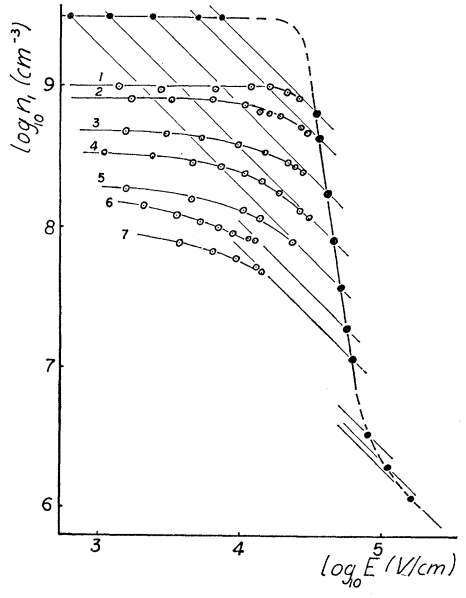

FIG. 11. Neutrality density of electrons n_1 in regions P and R, and n_s (curves 1–7) in region Q. The curves 1–4 correspond to 1–4 in Figs. 4–6.

[20] Here a transition occurs from a region in which the solution lies below $n_1(E)$ (solid arrows symbolize the field of directions) to a region in which the solution lies above $n_1(E)$ [here $n_s(E)$]. For the latter region, the field of direction is symbolized by dashed arrows.

[21] The minimum-entropy-production criterion is not needed for determination of this stationary solution, since the current is uniquely determined by the boundary conditions.

adjacent to Q. The solution is indicated by the arrow in Fig. 9 and has a shape as given by curve b in Fig. 10. For comparison, the solution for low applied voltages as given in Fig. 8 and discussed before is pictured by curve a in Fig. 10.

With further increasing voltage, the solution comes closer to the singular point II, and hence the width of the high-field domain in R grows, as discussed in Sec. 2 for the homogeneous-excitation case. The electron density $n_s(E_{I^*})$ controls the saturation current and therefore determines the electron density at the boundary between Q and R, which, in good approximation, is given by n_{II} (Fig. 9). Changing n_s by variation of the excitation in region Q changes n_{II}.

Using Eq. (4), $n_s(E)$ for different illuminations in region Q (see Fig. 11) is obtained from the measured current-voltage characteristics (some of which are given in Fig. 4). In Fig. 11, $n_2(E)$ as determined by j is also drawn. This shows that E_{I^*}, i.e., the field in region Q, lies markedly below E_{II} (see also Fig. 10), in agreement with the discussion given above. Figure 11 also shows that the mobility is nearly field-independent up to at least 17 kV/cm (see curve 1). The decrease of $n_s(E)$ with field at lower-field values for stronger quenching (curves 2–7) can be explained by field-enhanced ionization of sensitizing centers. This and the general behavior of $n_1(E)$ will be discussed in more detail in a future paper.

ACKNOWLEDGMENTS

We would like to acknowledge the growing of the CdS platelets by L. van den Berg and the construction of the crystal holder by M. Weaver and E. E. Riley.

PHYSICAL REVIEW VOLUME 169, NUMBER 3 15 MAY 1968

Infrared Spectral Emittance and Optical Properties of Yttrium Vanadate

H. E. Rast, H. H. Caspers, and S. A. Miller
*Infrared Division, Research Department, Naval Weapons Center Corona Laboratories**
Corona, California 91720

(Received 13 November 1967)

The infrared spectral emittance E of single scrystals of YVO_4 has been examined near 4.2 and 77°K in the wavelength range 4–125 μm. Of the expected seven active transverse optical modes at $\mathbf{k}\sim 0$, six have been observed and assigned to their symmetry species based on their polarization with respect to the crystalline axes. The observed frequencies of the transverse optic E_u modes were 196, 261, and 788 cm^{-1}; and for A_{2u} modes, 310, 455, and 803 cm^{-1}. The relation between emittance and reflectance, $E=1-R$ in the opaque region of lattice vibrations, permits one to determine the reflectance R. By least-square-fitting the reflectance data to an independent set of damped harmonic oscillators, infrared dispersion parameters were determined for the E_u vibrations.

INTRODUCTION

RECENTLY, some interest has arisen in yttrium orthovanadate as a medium for spectroscopic studies of rare-earth ions and as a host material for lasers.[1–4] It is natural, therefore, to investigate the lattice vibrations of YVO_4 and to determine the optical properties and the extent to which the phonon spectrum might influence the spectral properties of doped rare-earth ions. In a previous report,[5] the crystal structure of YVO_4 was analyzed group-theoretically to predict the expected $\mathbf{k}=0$ lattice vibrations, and the experimental Raman spectrum was presented. In the work presented here, we examine the infrared spectrum of YVO_4 and correlate the observed data with the results of the Raman spectrum. Finally, the determination of the optical constants is discussed.

Lattice Vibrations of YVO_4

The crystal structure of YVO_4 is isomorphic to zircon, having space-group symmetry D_{4h}^{19}. Figure 1 depicts this tetragonal crystal structure and illustrates the primitive cell. With two molecules per primitive cell, this structure gives rise to 36 vibrational modes at $\mathbf{k}=0$, including crystal translations. The group-theoretical analysis of the lattice vibrations was carried out in great detail elsewhere[5] and will not be repeated here. Instead, we summarize the results of that analysis in Table I by including the number, symmetry, and activity of the expected motions under D_{4h} symmetry. Only seven of these modes are infrared active: Three

* Formerly Naval Ordnance Laboratory, Corona, Calif.

[1] C. Brecher, H. Samelson, A. Lempicki, R. Riley, and T. Peters, Phys. Rev. **155**, 178 (1967).
[2] J. R. O'Connor, Appl. Phys. Letters **9**, 407 (1966).
[3] W. Wanmaker, A. Bril, J. ter Vrugt, and J. Broos, Philips Res. Rept. **21**, 270 (1966).
[4] A. K. Levine and F. C. Palilla, Appl. Phys. Letters **6**, 118 (1964).
[5] S. A. Miller, H. H. Caspers, and H. E. Rast, Phys. Rev. **168**, 964 (1968).

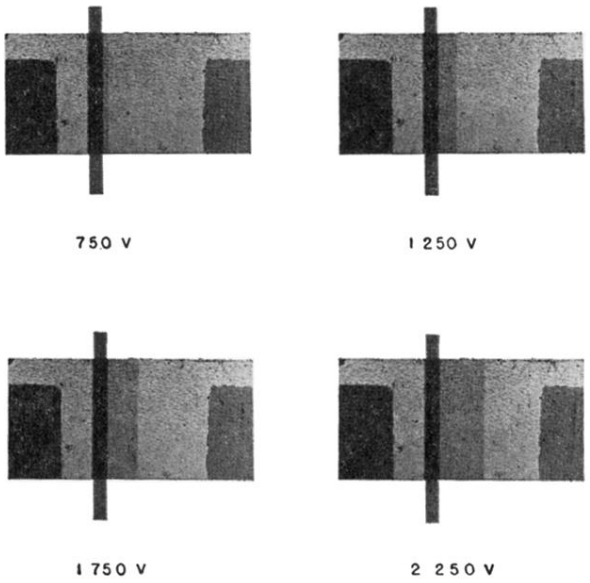

FIG. 5. Photographs in monochromatic light (507 nm) of CdS platelet with shadow, showing the high-field domain increasing in width in region *R* adjacent to the shadow, for increasing voltages applied to the crystal (cathode at the left side).